APPLIED MECHANICS

З можливого різноманіття технологічних дефектів стільникового заповнювача, що впливають на його фізико-механічні характеристики, одним з найбільш істотних постулюється початковий технологічний погин граней його чарунки. Стаття присвячена дослідженню впливу технологічного погину граней стільникового заповнювача на його фізико-механічні характеристики, що забезпечує стабілізацію його якості і, відповідно, експлуатаційних характеристик конструкцій на його основі. На відміну від існуючих робіт, було розглянуто дискретно-елементну модель стільників. Стільниковий заповнювач був представлений у вигляді конструкції, що складається з різних елементів: граней одинарної фольги, граней з двох склеєних шарів фольги та фіктивних ребер – кутових стикових зон двох сусідніх граней. Досліджено процес послідовної втрати несучої здатності елементами чарунки стільникового заповнювача при поперечному стисненні та поздовжньому зсуві. Такий аналіз поведінки окремих елементів чарунки стільників при наявності в них початкового технологічного погину дозволив врахувати особливості роботи кожного з них шляхом побудови відповідної типу навантаження діаграми деформування заповнювача. На підставі цього розроблено підхід, що дозволяє прогнозувати характер роботи стільникового заповнювача з урахуванням особливостей сприйняття навантаження окремими елементами чарунки стільників при наявності в них початкового технологічного погину. Дано рекомендації до використання отриманих результатів в рамках запропонованих в ряді робіт підходів до оптимізації за масою проектних параметрів стільникових конструкцій. Рекомендації дозволяють синтезувати модуль перевірочного блоку оптимізації, в якому дається висновок про несучу здатність оптимального за масою варіанту сендвічевой конструкції зі стільниковим заповнювачем з урахуванням наявності в його гранях початкового технологічного погину в межах регламентованого допуску. Такий синтез на сучасному рівні технології виробництва стільникового заповнювача дозволить в результаті реалізувати практично вичерпні можливості цього типу заповнювача і конструкцій на його основі

Ключові слова: сендвічеві конструкції, стільниковий заповнювач, фізико-механічні характеристики, технологічний погин граней стільників

UDC 629:539.3
DOI: 10.15587/1729-4061.2019.179258

EFFECT OF TECHNOLOGICAL CAMBER IN THE FACETS OF A CELLULAR FILLER ON ITS PHYSICAL AND MECHANICAL CHARACTERISTICS

A. Kondratiev
Doctor of Technical Sciences,
Associate Professor, Head of Department*
E-mail: a.kondratiev@khai.edu
T. Nabokina
PhD, Associate Professor*
E-mail: t.nabokina@khai.edu
*Department of
Rocket Design and Engineering
National Aerospace University
Kharkiv Aviation Institute
Chkalova str., 17, Kharkiv, Ukraine, 61070

Received date 26.08.2019
Accepted date 16.09.2019
Published date 05.10.2019

1. Introduction

One of the priority areas for choosing rational design-force schemes for assemblies of various purposes is the widespread use of sandwich-type structures [1, 2]. Elements of these structures consist of two bearing sheathings and a filler of different configuration between them [3, 4]. Extending the scope of application of such structures in various fields of technology has been made possible by the increased use of polymeric composite materials in them [5–7]. This type of a structural-force scheme makes it possible to implement some of the highest indicators of specific strength and rigidity at a minimum mass, which is the defining criterion for the efficiency of assemblies in different technological classes.

One of the most common types of a filler is the cellular one, with a cell of the proper hexagonal shape [10, 11]. Its basis is typically an aluminum foil, polymeric paper, or fiberglass [12, 13]. Currently, the most widely used is the cellular filler made from metallic foil, manufactured mainly by gluing methods [12, 14]. Such a filler has the largest manufacturability, it possesses high specific rigidity and strength characteristics.

Results from testing cellular structures show that destruction typically occurs before the estimated load value is reached due to the destruction of the weakest link, the cellular filler [4, 12, 15]. This is due to the presence of all sorts of technological deviations, which inevitably occur in the manufacture of cellular fillers within certain technical conditions and tolerances [16]. The curvilinear character of cell walls can be predetermined at the stage of obtaining a sheet (flat) workpiece, which is received by the methods of rolling and straightening a sheet material. This workpiece can then be used to fabricate a cellular filler, as shown in paper [17].

This pronounced technological heredity of cellular fillers leads to integrated changes in the projected properties of honeycomb structures and deviations in the carrying capacity of cellular structures, exceeding the permissible (regulated) ones [16, 18].

Ensuring the maximum carrying capacity of the cellular filler, as the weakest link of a given class of structures, requires a detailed accounting of the estimated level of its physical and mechanical characteristics, taking into consideration the technology of its manufacture.

2. Literature review and problem statement

The nature of the cellular filler as a structural material is complex. In essence, it is a discrete structure consisting of interconnected regularly repeated plates of a single layer of foil and two layers with an adhesive layer (Fig. 1) [3, 4, 12].

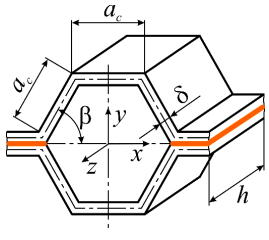

Fig. 1. Cellular filler with the accepted coordinate system

In determining the physical-mechanical characteristics, cellular filler is typically considered to be a conditional, equivalent in operation, homogeneous in volume, orthotropic filler. The characteristics of such a filler depend on the geometric configuration of the honeycomb cell, the thickness of the foil, the physical and mechanical characteristics of a material that the cellular filler is made from, and the level and nature of applied loads [3, 4]. Calculations and tests have established that for the cellular filler the main elastic characteristics are the elasticity module in the direction perpendicular to bearing sheathings – E_z and shear modules in the planes of cell facets – G_{xz} and G_{yz}. [3, 4, 12]. The magnitudes for other elastic and shear modules are negligible and are typically not taken into consideration in the calculations [10, 11].

Values of the physical-mechanical characteristics of the cellular filler significantly depend on patterns in the load perception by the individual elements of a honeycomb cell [19, 20]. Thus, the result of the gradually increasing load on cells is a consistent loss of the carrying capacity of its constituent elements. Based on model [21], paper [20] considered the effect of loss of stability by cell facets at shear on the corresponding physical and mechanical characteristics of the cellular filler.

However, studies into the physical and mechanical characteristics of cellular fillers are still relevant. In most cases, depending on the degree of importance of a structure, conclusion about the magnitudes for the physical and mechanical characteristics of cellular fillers is made based only on the results from processing data on tests [3, 4, 16].

Attempts to achieve a satisfactory convergence between theoretical and experimental data on the physical and mechanical characteristics of cellular fillers come down to refining existing mathematical models of honeycomb structures at the expense of their technological imperfections [22–28].

Paper [22] reports results of research on accounting, in the design of cellular structures, of technological imperfections of honeycomb structures. A procedure for optimizing the tolerances in the manufacture of a cellular filler for a panel, which ensures the predefined bearing capacity of the structure, has been proposed. However, the suggested approach to regulating tolerances for the parameters of a honeycomb structure cell shape is aimed at ensuring the regulated deviation in the carrying capacity of a particular cellular structure.

Paper [23] reports results from a study into ensuring the physical and mechanical characteristics of cellular fillers for cases when its characteristics go beyond permissible values due to certain deviations in the geometry of honeycomb structures. The results obtained have eventually made it possible to improve the standard industrial processes in the fabrication of honeycomb structures. However, it is not possible to establish a specific mechanism of influence of technological imperfections of a cellular filler on its physical and mechanical characteristics.

Papers [24, 25] address the development of scientifically-substantiated methods for regulating the margins of tolerance for technological parameters of the basic operations in the production of honeycomb structures and for defects. However, the cited papers do not take into consideration a series of issues that could have a significant impact on the results and require separate studies. Thus, these papers indicate that of the possible variety of technological defects of the cellular filler that affect its physical and mechanical characteristics, one of the most critical is the technological camber of the facets of cells in honeycomb structures. It is pointed out that the mechanism of the origin of the initial technological cambers of cell facets and their quantification have remained not only unexplored, but also not defined. It is concluded that the difficulty of solving this task is due, on the one hand, to the small values of cambers themselves of the same order (and less) with the thickness of the foil, and, on the other hand, with the uncertainty and multifactorial nature of the mechanism of their occurrence.

In this regard, the approach has been applied up to now, proposed in [21] and further developed in [25, 26], based on setting the values for technological cambers and subsequent determination, at these values, of the physical-mechanical characteristics of a cellular filler. At the same time, papers [25, 26] consider the issue on determining elasticity modules for the case when the elements of honeycomb structures have the initial camber in the form of a "cap". The following assumptions were accepted. The camber was presented as a single wave along and across the plate of a honeycomb cell. Rigidity of the honeycomb elements was evenly distributed across the surface of outer layers. The presence of the initial camber of the facets of cells in honeycomb structures was reduced to a factor of reducing their stiffness for compression ξ. As a result, the following dependence was derived to determine the cross-sectional elasticity module of a cellular filler at compression, taking into account the initial camber of elements in its honeycomb cells:

$$E_z = \frac{2\delta\xi_1 E_c + 2\delta\xi_2 E_c}{2.6a_c}, \quad (1)$$

where δ is the thickness of a honeycomb material, E_c is the elasticity module of a foil material, a_c is the width of the dual cell.

The coefficients ξ_i are determined from the plot built for unattached longitudinal edges of single or double plates the honeycomb elements at the onset of loading an appropriate plate with an initial camber [21]. The discrepancy between the theoretical value for the honeycomb elasticity mod-

ule at cross-compression and that experimentally determined [25, 26] is larger than 4 times. In addition, papers [25, 26] suggested that should the honeycomb elements have the initial camber in the form of a "cap", it would only affect the operation of a honeycomb cell's element at compression and should not significantly impact their operation at shear. Thus, the discrepancy, reported in papers [25, 26], between the theoretical and experimental values for the physical and mechanical characteristics of a cellular filler is related largely to the qualitative assessment of a specific production technology of honeycomb structures.

An attempt to solve the task on establishing the mechanism of influence of the technological camber of the facets of a cellular filler on its physical and mechanical characteristics by considering the new discrete-element model of honeycomb structures was undertaken in studies [12, 27, 28]. However, the results obtained do not fully reflect the entire range of patterns in the perception of loads by individual elements of a honeycomb cell in the presence of the initial technological camber in them, which also requires further research.

An effective alternative to the field tests of actual experimental samples on determining the physical and mechanical characteristics of fillers is the use of information technology involving a finite-element analysis [29, 30]. Modern tools of engineering analysis make it possible to find the strained-deformed states of sandwich-type structures directly, without replacing the filler used with some solid orthotropic material, that is without its "smearing" [31, 32]. However, the labor intensity of such an approach seems to be justified only if verification calculations are necessary [8, 12, 32]. In practice, designers have always used, and still do, the analytical models for sandwich-type structures. Such models make it possible to theoretically calculate the reduced physical and mechanical characteristics of fillers, expressed through their geometric parameters and the properties of the material that they are made from [8, 12, 32].

The use of these models, while enabling the derivation of an approximate result, mostly allow the subsequent adjustment of the result [13, 18, 23]. These models, as well as the expressions they implement to determine the physical and mechanical characteristics of fillers, continue to be a reliable and effective means of optimizing the parameters of sandwich-type structures.

Thus, the cellular filler is lacking a sufficiently developed approach, enabling the prediction of the nature of its operation, taking into consideration patterns in the perception of load by individual elements of honeycomb structures in the presence of the initial technological camber in them.

Existence of such an approach would make it possible to take into consideration significant deviations in the physical-mechanical characteristics of honeycomb structures, observed in experiments, from those determined from known analytical models [3, 4, 21].

3. The aim and objectives of the study

The aim of this work is to establish the mechanism of influence of the technological camber of the facets of a cellular filler on its physical and mechanical characteristics, which could ensure the stabilization of quality and operational characteristics of honeycomb structures, as well as the structures based on them.

To achieve the set aim, the following tasks have been solved:

– for the gradual loading with cross-compression and shear in a cellular filler, to analyze the performance of certain elements in its cell in the presence of the initial technological camber in them;

– to construct an approach that would make it possible to predict the character of operation of the cellular filler, taking into consideration patterns in the perception of load by individual elements of the honeycomb cell in the presence of the initial technological camber in them within the regulated tolerance.

4. Materials and research methods

When implementing our proposed discrete-element model of the representative element of a cellular filler under a gradual loading at compression and shear, the methods and mathematical models from the mechanics of a deformable solid body in elastic statement have been employed. Proof of the validity of our conclusions is the adequacy of estimated models and data, which allowed us to quantify the impact of the technological camber in the cellular filler facets on its physical-mechanical characteristics, previously observed in experiments only. When comparing the proposed approach with experimental data, we have considered the aluminum cellular filler with a regular hexagonal cell, 13.5 mm high, with the size of the cell facet of 5 mm, the thickness of the foil 0.03 mm, and the initial technological camber of facets of 0.15 mm.

5. Determining the physical-mechanical characteristics for a cellular filler under gradual loading by transverse compression

Specific factors that determine the emergence of the technological camber of a cellular filler's cells from a metallic foil, obtained by gluing to the carrier sheathings, are substantiated in papers [16, 26, 33]. In accordance with the proposed classification of defects in honeycomb structures, formed during the formation of a cellular packet, their primary manifestations were considered. The defects are associated with the emergence of foil deformations when the glue shrinks and with a significant difference in the coefficients of linear thermal expansion of the foil and glue. The use of recommendations from paper [33] on the margins of tolerances for the magnitude of a given technological camber makes it possible to assess its impact on the physical-mechanical characteristics of a cellular filler by significantly refining the discrete-element model of honeycomb structures, proposed earlier in papers [27, 28]. To take into consideration patterns in the perception of transverse compressive and longitudinal shear loads by individual elements of a honeycomb cell in the presence of technological camber in their facets, we shall consider part of the area of a carrier sheathing (Fig. 2). The area of the selected part of the carrier sheathing is equal to

$$F_{\Sigma} = \left(2a_c + 2a_c \cos\beta\right)\left(3a_c \sin\beta\right) = 6a_c^2\left(1+\cos\beta\right)\sin\beta. \qquad (2)$$

Let us highlight its corresponding representative element of the cellular filler with a hexagonal cell of height h whose model is shown in Fig. 3. A given representative ele-

ment of a honeycomb structure is actually composed of six facets of a single foil and three twin facets of foil, obtained by gluing together two layers of foil (Fig. 3).

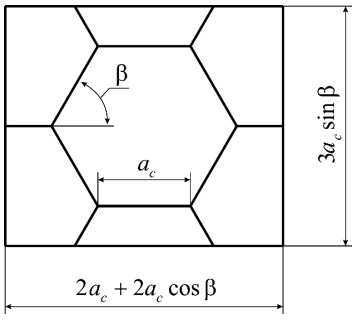

Fig. 2. Dimensions of the cross-sectional area of the representative element of a cellular filler

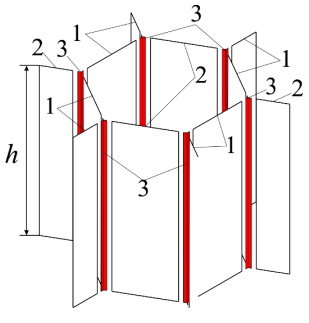

Fig. 3. Model of the representative element of a cellular filler without the initial technological camber of the facets of its cells: 1 — facets of single foil; 2 — facets of two glued layers of foil; 3 — imaginary edges

Following the recommendations from papers [28, 33] for the margins of tolerances for the magnitude of the initial technological camber of honeycomb facets, we set the arrow of this camber f_0 for the facet of single foil. The twin facets of foil, which are obtained by gluing together two layers of foil, will be considered without any initial imperfections. Let us represent a discrete model of the representative element of a cellular filler (Fig. 4) in the following form:

– the facets of single thickness will be replaced with plates, thickness of δ, with the arrow of the initial technological camber f_0; referred to as the type I facets (Fig. 4, *a*);

– the facets of double thickness will be replaced with plates, thickness of 2δ; referred to as the type II facets (Fig. 4, *b*);

– in the regions of a foil bend, we shall place imaginary edges, which consist of parts of the plates of facets "attached" to each edge, which have the same compression stresses as the strains in the imaginary edges (Fig. 4, *c*).

The geometric dimensions of the cross section of an imaginary edge (Fig. 5) are as follows: thickness of the "attached" parts of plates of honeycomb cell facets – δ and 2δ, their width, respectively, for parts of the type I and II facets is Δ_1 and Δ_2.

To reflect the character of operation of a cellular filler under a phased load, taking into consideration the presence of the initial technological camber in its facets, it would suffice to know the law of changes in stresses in it depending on deformations.

To this end, we shall build deformation diagrams $\sigma_z - \varepsilon_z$, $\tau_{xz} - \gamma_{xz}$ and $\tau_{yz} - \gamma_{yz}$ for a conditional homogeneous filler, equivalent to a cellular one, taking into consideration the patterns in the perception of a corresponding loading by individual elements of a honeycomb cell and the related physical phenomena. The reduced modules of normal elasticity E_z and shear G_{xz}, G_{yz} for honeycomb structures at any time of loading will be equal to the tangent of the tangent's inclination angle at a point to the corresponding diagram of the built dependence at the corresponding magnitude of deformation of a cellular filler.

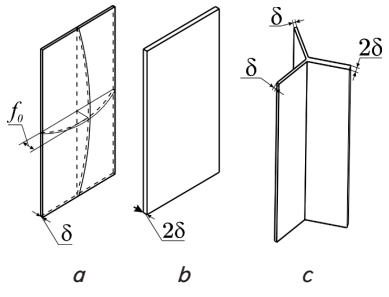

Fig. 4. Elements of the discrete-element model of the representative element of a cellular filler: *a* — type I facet; *b* — type II facet; *c* — imaginary edge

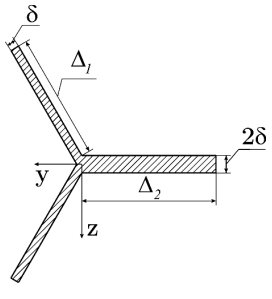

Fig. 5. Cross-section and local coordinates system of an imaginary edge of the representative element of a cellular filler

To take into consideration the pattern of perception of the transverse compressive loading by individual elements of a honeycomb cell and the accompanying physical phenomena, we shall consider work of the representative element of a cellular filler, which is loaded with a gradually increasing transverse load. As a result of its action, each element of the structure of a cellular filler undergoes identical deformations, equal to the total deformation of honeycomb structures ε, at different levels of stresses. So, in the type I facet – these are stresses σ_1, in the type II facet – σ_2, in imaginary edges – σ_3. Their magnitudes in the process of growth of the transverse compressive loading gradually reach those values at which the flat form of equilibrium of the components of the discrete model of the representative element becomes unstable. In this case, they lose stability, which can be regarded as exhaustion of carrying capacity. In this case, the first to lose the stability are the type I facets, next – the type II facets. It is obvious that for the type I facets, which have the initial technological camber, compressive efforts will not cause the loss of a flat form of equilibrium, because the compressive efforts will only increase the arrow of the full bend of the plate by increasing the arrow of elastic one. The result of reaching a critical condition by the type II facets

and due to the inability of the type I facets to redistribute the increasing load, the operation of honeycomb structures "give rise" to imaginary edges. The loss of stability of these edges results in the exhaustion of the carrying capacity of the entire cell, and, therefore, the cellular filler in general.

Let us specify two stages in the operation of the representative element of honeycomb structures: before and after the incorporation of imaginary edges into operation.

At the first stage, the load acting in the representative element of area F_Σ is equal to the sum of loads acting in the types I and II facets, as there are no imaginary edges:

$$N_\Sigma = 6N_1 + 3N_2, \tag{3}$$

where N_Σ is the total load in the representative element, acting in the reduced filler, equivalent to a cellular one; N_1 is the load that acts in the type I facet; N_2 is the load acting in the type II facet.

To determine the critical stresses of loss of stability for the type II plate, we shall use the Euler formula [34]:

$$\sigma_{cr2} = K\frac{\pi^2 D}{a_c{}^2\delta_{II}}, \tag{4}$$

where σ_{cr2} are the critical stresses of loss of stability by Euler in the type II facet; K is a factor that depends on the relationship between the sides of a cell's facet and the conditions of its leaning; $\delta_{II}=2\delta$ is the thickness of the plate under consideration (type II facet);

$$D = \frac{E_c\delta_{II}^3}{12\left(1-\mu_c{}^2\right)}$$

is the cylindrical rigidity of the plate under consideration; μ_c is the Poisson coefficient for a material that the foil is made from.

Since the type II facet is deformed in line with the linear Hook law, the deformation of the cellular filler, corresponding to the critical stress of loss of stability, will be determined as follows:

$$\varepsilon_{cr2} = \frac{\sigma_{cr2}}{E_c}. \tag{5}$$

The presence of the initial camber in the type I facet changes the character of its operation: it is deformed not by the linear Hook law, but in line with an unknown non-linear one. It is difficult to describe such behavior analytically. To define the deformation law of the type I facet, we shall determine stresses and deformation of a given plate, taking into consideration the initial camber in the following way.

As a result of the impact from the compressive transverse load on the elements of a cell of the cellular filler, the considered type I facet is loaded with an evenly distributed compression effort N_x, which creates stress σ_1 1 in the middle plane of a given facet. Fig. 6 shows the considered type I plate, loaded with an evenly distributed compression effort N_x.

When a given plate is exposed to the action of an evenly distributed compressing effort N_x, there emerges an elastic deflection w_1. A complete deflection w at any point at the middle surface of the type I facet in this case will be equal to the amount of the elastic and initial technological camber: $w=w_1+w_0$. Let us apply the equilibrium equation for a plate from paper [35]:

$$D\left(\frac{\partial^4 w}{\partial x^4} + 2\frac{\partial^4 w}{\partial x^2\partial y^2} + \frac{\partial^4 w}{\partial y^4}\right) = q + \left(N_x\frac{\partial^2(w)}{\partial x^2} + N_y\frac{\partial^2(w)}{\partial y^2} + 2N_{xy}\frac{\partial^2(w)}{\partial x\partial y}\right), \tag{6}$$

where w is a function of the complete deflection of a plate; N_x, N_y, N_{xy} are the efforts, acting in the middle plane of the plate, distributed over its width, respectively, normal and cutting; q is the transverse load acting on a plate.

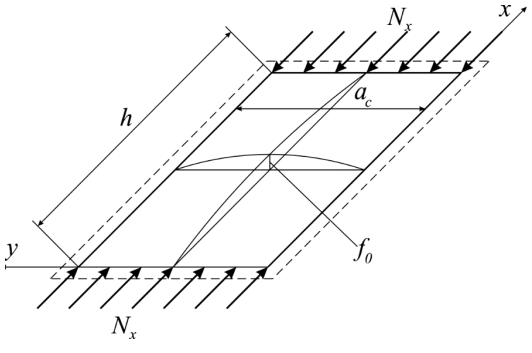

Fig. 6. The type I facet under consideration, loaded with an evenly distributed compression effort N_x, caused by the transverse compression load on the representative element of a cellular filler

To take into consideration the initial imperfection of the type I facet, we accept in the right-hand side of equilibrium equation (6) that the complete deflection is equal to $w=w_1+w_0$. The left-hand side of equation (6) was derived from the expression for bending momenta, as the latter depend not on the entire curvature of the plate, but only on its change; in this part we accept, instead of the full deflection w, the elastic deflection w_1 only. Thus, the equilibrium equation (6) for the case of a plate with the initial technological camber w_0 is transformed to the following form:

$$D\left(\frac{\partial^4 w_1}{\partial x^4} + 2\frac{\partial^4 w_1}{\partial x^2\partial y^2} + \frac{\partial^4 w_1}{\partial y^4}\right) = q + \left(N_x\frac{\partial^2(w_1+w_0)}{\partial x^2} + N_y\frac{\partial^2(w_1+w_0)}{\partial y^2} + 2N_{xy}\frac{\partial^2(w_1+w_0)}{\partial x\partial y}\right). \tag{7}$$

We shall consider the case of a loosely leaned plate when boundary conditions are satisfied if one takes expressions for the functions of the initial and elastic deflections in the form of double series for sinuses:

$$w_0 = \sum_m\sum_n f_{0mn}\sin\frac{m\pi x}{h}\sin\frac{n\pi y}{a_c};$$

$$w_1 = \sum_m\sum_n f_{1mn}\sin\frac{m\pi x}{h}\sin\frac{n\pi y}{a_c}, \tag{8}$$

where m and n are the summation indicators corresponding to the number of waves in the direction of the x, y axes, respectively; f_{0mn}, f_{1mn} are the amplitudes of functions of the initial and elastic deflections, represented in the form of double series for sinuses.

Believing that in the case of the load being considered $q=N_y=N_{xy}=0$, and considering that the acting compression effort is equal to $N_x=-\sigma_1\delta$, we shall substitute ex-

pressions (8) for deflections w_1 and w_0 in equation (7). As a result of the transforms, we shall obtain the following expression in a general form:

$$\pi^4 D\sum_m\sum_n\left(\frac{m^2}{h^2}+\frac{n^2}{a_c^{\,2}}\right)^2 f_{1mn}\sin\frac{m\pi x}{h}\sin\frac{n\pi y}{a_c}=$$
$$=\pi^2\delta\sigma_1\sum_m\sum_n\frac{m^2}{h_{c3}^{\,2}}\left(f_{1mn}+f_{0mn}\right)\sin\frac{m\pi x}{h}\sin\frac{n\pi y}{a_c}. \qquad (9)$$

By accepting the number of waves m and n to be equal to unity for the central point of the plate, we derive from expression (9) a dependence to determine the acting stress σ_1, taking into consideration the presence of the initial technological camber:

$$\sigma_1=\frac{\pi^2 D}{a_c^{\,2}\delta}\left(\frac{a_c}{h}+\frac{h}{a_c}\right)^2\frac{f_1}{f_0+f_1}. \qquad (10)$$

The deformation in the type I facet that emerges from the action of compressing effort N_x, given the presence of the initial technological camber arrow f_0 in it, will be derived geometrically. Fig. 7 shows the cross-section, at $y=a_c/2$, of the considered type I facet with the initial technological camber arrow f_0.

As a result of the action of compressing effort N_x, the height h of a cellular filler will change by magnitude Δh and will equal h_1 (Fig. 8). In this case, the arc length arc L, formed by the surface of the type I facet, before and after loading with effort N_x, will remain unchanged.

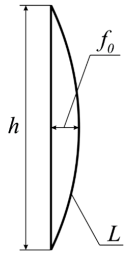

Fig. 7. Cross-section of the unloaded type I facet at $y=a_c/2$

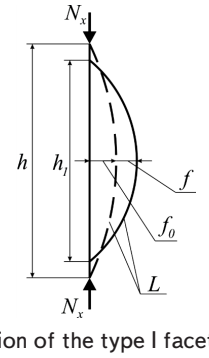

Fig. 8. Cross-section of the type I facet at $y=a_c/2$ under the action of a compressing effort

By accepting that a given arc is the arc of the circle, we shall express the arc length L before deformation through the honeycomb structure height h and the arrow of the initial camber f_0:

$$L=0.01745\frac{h^2+4f_0^2}{8f_0}\left(\frac{180}{\pi}2\arcsin\left(\frac{h}{2}\frac{8f_0}{h^2+4f_0^2}\right)\right). \qquad (11)$$

By expressing the arc length L after deformation through the honeycomb structure deformation ε and the arrow of complete flexure $f=f_0+f_1$, we obtain the following expression:

$$L=0.01745\frac{\left((1+\varepsilon)h\right)^2+4\left(f_1+f_0\right)^2}{8\left(f_0+f_1\right)}\times$$
$$\times\frac{180}{\pi}2\arcsin\left(\frac{(1+\varepsilon)h}{2}\cdot\frac{8\left(f_0+f_1\right)}{\left((1+\varepsilon)h\right)^2+4\left(f_1+f_0\right)^2}\right). \qquad (12)$$

By equating expressions (11) and (12), we obtain the following equation:

$$\frac{h^2+4f_0^2}{8f_0}\arcsin\left(\frac{h}{2}\frac{8f_0}{h^2+4f_0^2}\right)=$$
$$=\frac{\left((1+\varepsilon)h\right)^2+4\left(f_1+f_0\right)^2}{8\left(f_0+f_1\right)}\times$$
$$\times\arcsin\left(\frac{(1+\varepsilon)h}{2}\frac{8\left(f_0+f_1\right)}{\left((1+\varepsilon)h\right)^2+4\left(f_1+f_0\right)^2}\right). \qquad (13)$$

Solving equation (13) in the form of a dependence $\varepsilon=g(f_1, f_0, h)$ will make it possible to relate the magnitude of deformation of a cellular filler ε to the magnitude of arrow of elastic camber f_0, growing with the load, at a fixed value for the arrow of the initial camber f_0 and the honeycomb structure height h. Equation (13) refers to a class of equations that include a composition of direct and inverse functions. It is very difficult to obtain an analytical form of the function $\varepsilon=g(f_1, f_0, h)$ in this case. Fig. 9 shows the character of change in the function $\varepsilon=g(f_1, f_0, h)$ at a different magnitude of the initial technological camber arrow, regulated in accordance with the recommendations from paper [28, 33], in the range $0.4\delta\le f_0\le 1.4\delta$.

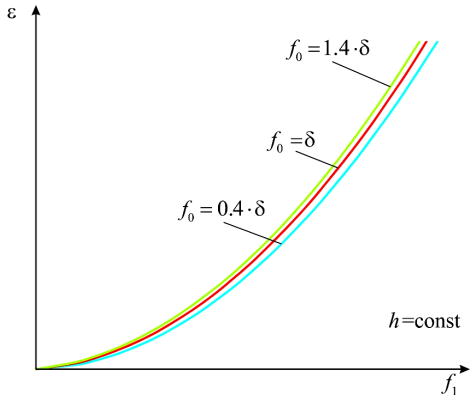

Fig. 9. The character of change in the function $\varepsilon=g(f_1, f_0, h)$ in the type I facet

For a series of values of elastic camber arrow f_1, by finding the magnitudes of the corresponding deformations ε and stresses σ_1, we shall define the law of deformation of the type I plate in a parametric form:

$$\begin{cases}\sigma_1=g\left(f_1,f_0\right);\\ \varepsilon=k\left(f_1,f_0\right).\end{cases} \qquad (14)$$

The character of change in the law of deformation of the type I facet, taking into consideration the arrow of the initial technological camber, is shown in Fig. 10.

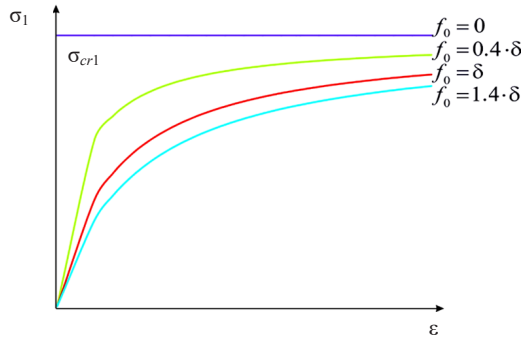

Fig. 10. The character of change in the law of deformation of the type I facet, taking into consideration the presence of the initial camber with an arrow f_0 in it

By guiding the arrow of the elastic camber to zero f_1=0 in expression (10), we shall obtain critical stresses for the loss of stability of the ideal facet of type I. It follows from the analysis of Fig. 10 that the level of acting stresses σ_1 in the type I facet with the initial camber is significantly reduced with the growth of its arrow f_0 compared to the corresponding critical stresses for the same ideal plate.

We shall find acting loads in the representative element and facets of types I and II at the first stage of operation of a cellular filler, that is before the onset of deformations in it, corresponding to the critical stresses of stability loss by the type II facets ε_{cr2}:

$$N_{red}=\sigma_{red}F_{\Sigma},\quad N_1=\sigma_1F_1,\quad N_2=\sigma_2F_2, \tag{15}$$

where σ_{red} are the stresses in the reduced filler, equivalent to a cellular one; $F_1=a_c\delta$, $F_2=2a_c\delta$ are the areas of the cross-section of the facet of types I and II.

Considering (3), (5) and (15), we shall express the stresses that operate in the representative element of the reduced filler, corresponding to a cellular one, by area F_Σ at the first stage of its operation:

$$\sigma_{red}(\varepsilon)^{(1)}=\frac{6\sigma_1(\varepsilon)F_1+3E_c\varepsilon F_2}{F_{\Sigma}}. \tag{16}$$

Let us look at the second stage of operation of a cellular filler. To determine the stresses of loss of stability by an imaginary edge, we shall use the Euler formula for a compressed rod [36]:

$$\sigma_{cr3}=\frac{\pi^2E_cJ_{\min}}{F_3(\nu h)^2}, \tag{17}$$

where $J_{\min}$ is the minimum momentum of inertia of the area of the transverse section of an imaginary edge; v is a factor that depends on the condition for leaning by an imaginary edge; $F_3=2\delta(\Delta_1+\Delta_2)$ is the area of the transverse section of an imaginary edge.

The minimum momentum of inertia of the imaginary edge cross-section is chosen as the smallest of the momenta of inertia relative to the OY and OZ axes, respectively (Fig. 5):

$$J_y=\frac{(2\delta)^3\Delta_2}{12}+2\frac{\Delta_1^3\delta}{3}\sin^2(\beta);$$

$$J_z=\frac{2\delta\Delta_2^3}{12}+2\delta\Delta_2\left(\frac{\Delta_2}{2}\right)^2+2\frac{\Delta_1^3\delta}{3}\sin^2\left(\frac{\beta}{2}\right). \tag{18}$$

Until the type II facet of the cell of a cellular filler has not lost stability, stresses throughout its width are distributed evenly. When the compression continues after the loss of stability by a facet, the stresses are unevenly distributed across its width: the increasing load is perceived mainly by the longitudinal imaginary edges and adjacent plots of the "attached" parts of the facet under stresses σ_{cr3}. The stress level in the middle part of the type II facet is little different from the critical values σ_{cr2} (Fig. 11, *a*). Strict theoretical description of a given behavior is a very difficult task. To simplify the calculations, the next assumption is accepted. The unknown law of distribution among the critical stresses of loss of stability by a cell facet σ_{cr2} and an imaginary edge with adjacent plots of a cell facet σ_{cr3} lengthwise the facet will be replaced with a step-wise one (Fig. 11, *b*).

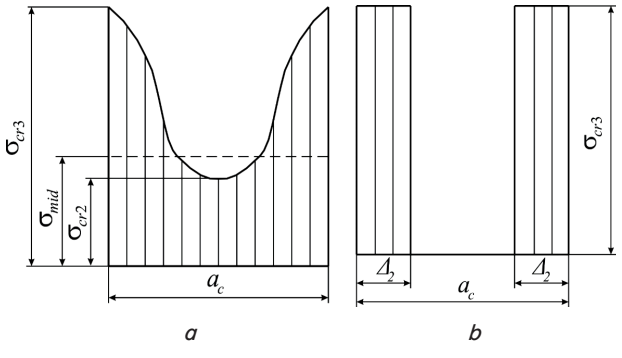

Fig. 11. Supercritical distribution of stresses in the type II facet: *a* – actual; *b* – equivalent, used in calculations

The width of the attached parts of the type II facet of the cell of a cellular filler will be determined from the condition of equality of force, perceived by the type II facet, the force it perceives, which operates with variable stresses at the same width. If one introduces the compressing stress $\sigma_{mid}=\sqrt{\sigma_{cr2}\sigma_{cr3}}$, average for the width of the type II facet, the result of the accepted assumption can be represented in the form

$$2\Delta_2\sigma_{cr3}=a_c\sigma_{mid}. \tag{19}$$

Thus, we obtain an expression to calculate the width of the part of the type II facet attached to the imaginary edge

$$\Delta_2=a_c\frac{\sqrt{\sigma_{cr2}\sigma_{cr3}}}{2\sigma_{cr3}}=\frac{a_c}{2}\sqrt{\frac{\sigma_{cr2}}{\sigma_{cr3}}}. \tag{20}$$

As regards determining the width of the attached part of the type I facet, it is not possible to choose this magnitude unequivocally. Theoretically, stresses across its width are evenly distributed. Hereafter, we assume that the width of parts of the facet of types I and II, attached to the edge, is equal, that is Δ_1=Δ_2. Because the dependence $\Delta_2(\sigma_{cr3})$ and the value σ_{cr3} are unknown, an iterative process is required. In the first iteration, we accept σ_{cr3}=σ_{02} (σ_{02} is the conditional yield point at the plastic deformation of 0.2 % of the

material that the honeycomb structures are made of). Next, we shall perform all the above calculations, which will result in a new value for the critical stresses of stability loss by edges σ^n_{cr3}. If the accuracy check

$$\frac{\sigma^n_{cr3}-\sigma_{cr3}}{\sigma^n_{cr3}}100\,\%\le 5\,\%$$

is not satisfied, we shall accept $\sigma^n_{cr3}=\sigma_{cr3}$, and calculate again. The process is terminated when the predefined accuracy is achieved. As the final values, we take Δ_2 and σ_{cr3}, derived during the last iteration.

The second stage of operation of a cellular filler is characterized by two possible "extreme" variants of behavior of its facets: the upper one, characterizing the maximum carrying capacity of the honeycomb representative element, and the lower one – minimum (Fig. 12).

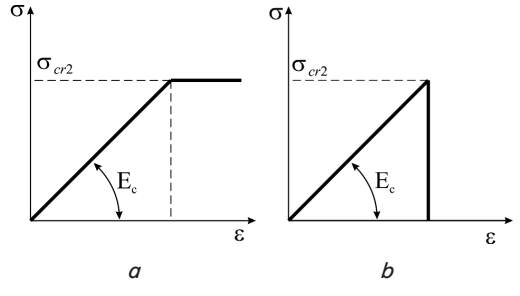

Fig. 12. Qualitative character of diagram $\sigma_2-\varepsilon$ for the type II facets in the supercritical zone: *a* – edges are not excluded from the operation completely; *b* – facets are excluded from operation completely

In the first case, the type II facets, having lost stability, are not excluded from the operation completely, and continue to carry a constant load corresponding to their critical stresses. The character of diagram $\sigma_2-\varepsilon$ for them will have a qualitative character shown in Fig. 12, *a*. In this case, the type I facets, without having a critical moment of operation, will continue to operate according to the non-linear law defined above. In this case, the load in the representative element of area F_Σ is equal to the sum of loads acting in the facets of types I, II and in an imaginary edge:

$$N_\Sigma=6N_1+3N_2+6N_3, \tag{21}$$

where $N_3=\sigma_3F_3$ is the load in an imaginary edge.

The stresses that emerging during the deformation of a cellular filler in an imaginary edge will be found according to the Hook law:

$$\sigma_3=E_c\varepsilon. \tag{22}$$

By transforming (21), we obtain the stresses acting in the representative element of the reduced filler, corresponding to a cellular one, of area F_Σ at the second stage of honeycomb operation:

$$\sigma_{red}(\varepsilon)^{(2)}_{\max}=\frac{6\sigma_1(\varepsilon)F_1+3\sigma_{cr2}F_2+6E_c\varepsilon F_3}{F_\Sigma}. \tag{23}$$

Otherwise, the type II facets are completely excluded from operation (Fig. 12, *b*). At the same time, the type I facets also cease to carry the load. In this case, the load that acts in the representative element of area F_Σ is equal to the load that acts in the imaginary edge. Formula (23) is converted into the following form:

$$\sigma_{red}(\varepsilon)^{(2)}_{\min}=\frac{6E_c\varepsilon F_3}{F_\Sigma}. \tag{24}$$

The true character of the cellular filler's behavior $\sigma_{redz}-\varepsilon_z$ at the second stage of operation will vary between values $\sigma_{red}(\varepsilon)^{(2)}_{\min}$ and $\sigma_{red}(\varepsilon)^{(2)}_{\max}$.

To build a deformation diagram $\sigma_{redz}-\varepsilon_z$ of a conditional homogeneous filler, equivalent to a cellular one, taking into consideration patterns in the perception of a corresponding load by individual elements of a honeycomb cell and the related physical phenomena, we shall use the following algorithm.

1. By following recommendations from papers [28, 33] for the predefined manufacturing technology of a glued sandwich-type structure with a cellular filler made of metallic foil, we set the arrow of the initial technological camber f_0.

2. By determining from formula (4) the value for a critical stress of the loss of stability by the type II facet σ_{cr2}, we find the corresponding deformation of honeycomb structures ε_{cr2} from formula (5).

3. For the deformation ε_{cr2}, by solving equation (13), we find the corresponding arrow of elastic flexure f_{cr2} for the plate of type I; by setting a series of values for elastic flexure $0\le f_1\le f_{cr2}$, we determine parametric functions $\varepsilon=g(f_1,f_0)$ and $\sigma_1=g(f_1,f_0)$ for the type I facet in the deformation range $0\le\varepsilon\le\varepsilon_{cr2}$.

4. For the resulting range of deformations $0\le\varepsilon\le\varepsilon_{cr2}$, based on dependence (16), we build a diagram $\sigma_{red}(\varepsilon)^{(1)}-\varepsilon$ that characterizes the performance of honeycomb structures before incorporating imaginary edges into operation.

5. By using formulae (17), (20), we conduct an iterative process to find the width of parts of the facets of cell Δ_1, Δ_2, attached to the edge, and the values for stress of loss of stability by an imaginary edge σ_{cr3}, as well as we find the corresponding deformation of honeycomb structures ε_{cr3} from a formula analogous to (5).

6. Similar to point 3, we determine functions $\varepsilon=g(f_1,f_0)$ and $\sigma_1=g(f_1,f_0)$ for the type I facet in the deformation range $\varepsilon_{cr2}\le\varepsilon\le\varepsilon_{cr3}\lim$.

7. To build the upper range of the diagram at the second section of operation of a cellular filler $\sigma_{red}(\varepsilon)^{(2)}_{\max}-\varepsilon$ (corresponding to the maximum carrying capacity of the representative element of a honeycomb structure) for the resulting range of deformations $\varepsilon_{cr2}\le\varepsilon\le\varepsilon_{cr3}$, we apply formula (23).

8. To build the lower range of the diagram $\sigma_{red}(\varepsilon)^{(2)}_{\min}-\varepsilon$ (corresponding to the minimum carrying capacity of the representative element of a honeycomb structure) for the resulting range of deformations $\varepsilon_{cr2}\le\varepsilon\le\varepsilon_{cr3}$, we employ formula (24).

Fig. 13 shows the qualitative character of the resulting diagram.

The strength limit of a cellular filler at transverse compression corresponds to the deformation of honeycomb structures when the carrying capacity of an imaginary edge is lost, that is its value lies between the upper and lower limits of the diagram $\sigma_{redz}-\varepsilon_z$ at $\varepsilon=\varepsilon_{cr3}$:

$$\frac{6E_c\varepsilon_{cr3}F_3}{F_\Sigma}\le\sigma_{ez}\le\frac{6\sigma_1(\varepsilon_{cr3})F_1+3\sigma_{cr2}F_2+6E_c\varepsilon_{cr3}F_3}{F_\Sigma}. \tag{25}$$

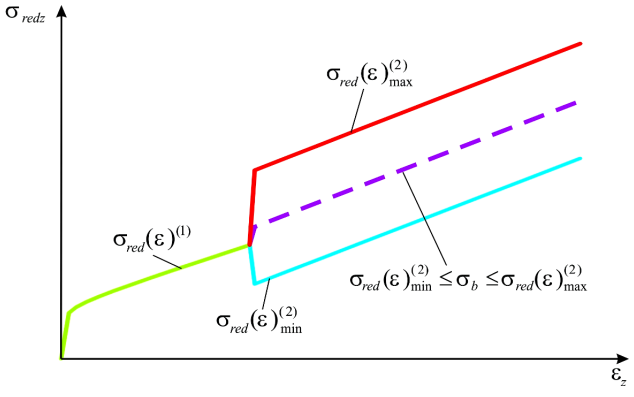

Fig. 13. Qualitative character of the cellular filler diagram $\sigma_{redz}-\varepsilon_z$, built considering the patterns in perceiving a transverse compression by individual elements of a honeycomb cell when there is an initial technological camber in its facets

As an example, the Table 1 below gives the results from comparing the proposed approach with experimental data for the initial technological camber of facets in a honeycomb cell f_0=0.15 mm [37]. The parameters for a cellular filler with a regular hexagonal cell: height, h=13.5 mm; size of the cell, a_c=5 mm; foil thickness, δ=0.03 mm; the elasticity module of the foil material, E_c=69,000 MPa.

Table 1

Comparison of theoretical magnitudes of cellular filler elasticity modules under transverse compression with experimental data

Experiment	Theoretical models			
[37]	[21] excluding the imperfections of the foil	[21, 25, 26] considering the imperfection of the foil	proposed approach (plots before and after the inclusion of honeycomb imaginary edges)	
E_{-Z}, MPa	E_{-Z}, MPa	E_{-Z}, MPa	E_{-Z}, MPa	
68–106	637	430	114	26

The results of this example confirm a better convergence between theoretical results with experimental results compared to existing analytical models.

6. Determining the physical and mechanical characteristics of a cellular filler under gradual loading by a longitudinal shear

We shall consider a discrete model of the representative element of a cellular filler, which is exposed to the effect of the cutting force Q_z, causing the shear of honeycomb structures in the planes of the facets of their foil. The physical phenomena associated with the perception of a given load are similar to transverse compression: at the smallest magnitude of this load, the stability is lost by the type I facets; the final destruction of honeycomb structures will be characterized by the loss of stability by the type II facets.

As a result of action of cutting force Q_z, the facets of honeycomb structures are loaded in the middle planes by evenly distributed cutting f efforts, which create in the middle planes of these facets the tangent stresses: in a type I facet – τ_1, in a type I facet – τ_2. Consider a type I facet exposed to the action of evenly distributed cutting effort N_{xy} (Fig. 14).

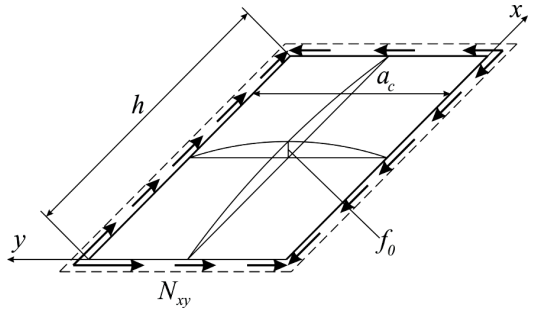

Fig. 14. The type I facet under consideration, which is loaded with an evenly distributed cutting effort N_{xy}, caused by the cutting force Q_z acting on the representative element of a honeycomb structure

Believing that under the considered load $q=N_x=N_y=0$, and accounting for that the cutting effort acting in the type I facet is equal to $N_{xy}=\tau_1\delta$, the equilibrium equation (6) will take the following form:

$$\pi^4 D\sum_m\sum_n\left(\frac{m^2}{h^2}+\frac{n^2}{a_c^2}\right)^2 f_{1mn}\sin\frac{m\pi x}{h}\sin\frac{n\pi y}{a_c}=$$
$$=\frac{2\pi^2\delta\tau_1}{ha_c}\sum_m\sum_n mnf_{1mn}\cos\frac{m\pi x}{h}\cos\frac{n\pi y}{a_c}+$$
$$+\frac{2\pi^2\delta\tau_1}{ha_c}\sum_m\sum_n mnf_{0mn}\cos\frac{m\pi x}{h}\cos\frac{n\pi y}{a_c}. \quad (26)$$

By applying the Bubnov-Galerkin procedure to equation (26), we shall obtain the following equation [34]:

$$\int_0^{a_c}\int_0^{h}\left(\pi^4 D\sum_m\sum_n\left(\frac{m^2}{h^2}+\frac{n^2}{a_c^2}\right)^2 f_{1mn}\sin\frac{m\pi x}{h}\sin\frac{n\pi y}{a_c}-\right.$$
$$-\frac{2\pi^2\delta\tau_1}{ha_c}\sum_m\sum_n mnf_{1mn}\cos\frac{m\pi x}{h}\cos\frac{n\pi y}{a_c}-$$
$$\left.-\frac{2\pi^2\delta\tau_1}{ha_c}\sum_m\sum_n mnf_{0mn}\cos\frac{m\pi x}{h}\cos\frac{n\pi y}{a_c}\times\right.$$
$$\left.\times\sum_p\sum_q\sin\frac{p\pi x}{h}\sin\frac{q\pi y}{a_c}\mathrm{d}x\mathrm{d}y=0\right. . \quad (27)$$

To integrate expression (27), we first derive the following integral:

$$\frac{1}{ha_c}\int_0^{a_c}\int_0^{h}\cos\frac{m\pi x}{h}\sin\frac{p\pi x}{h}\cos\frac{n\pi y}{a_c}\sin\frac{q\pi y}{a_c}\mathrm{d}x\mathrm{d}y. \quad (28)$$

Taking into consideration that for any integer m, n, p, q expressions

$$\sin m\pi=\sin n\pi=\sin p\pi=\sin q\pi=0,$$

the integral from expression (28) is

$$\frac{1}{ha_c}\int_0^{a_c}\int_0^{h}\cos\frac{m\pi x}{h}\cdot\sin\frac{p\pi x}{h}\cdot\cos\frac{n\pi y}{a_c}\cdot\sin\frac{q\pi y}{a_c}\mathrm{d}x\mathrm{d}y=$$
$$=\frac{(-p+\cos p\pi\cos m\pi)(-q+\cos n\pi\cos q)}{\pi^2(m^2-p^2)(n^2-q^2)}. \quad (29)$$

It is obvious that should $(m\pm p)$ and $(n\pm q)$ accept even values, the expression (29) turns to zero. Hence, it follows that $(m\pm p)$ and $(n\pm q)$ can only accept odd values; the expression (28) will take the form

$$\frac{1}{ha_c}\int_0^{a_c}\int_0^{h}\cos\frac{m\pi x}{h}\sin\frac{p\pi x}{h}\cos\frac{n\pi y}{a_c}\sin\frac{q\pi y}{a_c}\mathrm{d}x\mathrm{d}y=$$
$$=4\frac{pq}{\pi^2(m^2-p^2)(n^2-q^2)}. \quad (30)$$

By computing the remaining integrals in expression (27), we obtain the following equation:

$$\frac{\pi^4 ha_c D}{32\delta\tau_1}\left(\frac{m^2}{h^2}+\frac{n^2}{a_c^2}\right)^2 f_{1mn}-$$
$$-\sum_p\sum_q\left(f_{0pq}+f_{1pq}\right)\frac{mnpq}{(m^2-p^2)(n^2-q^2)}=0. \quad (31)$$

By recording ratio (31) for each combination of m, n, we obtain two systems of equations, one of which contains only terms with even sums $m+n$, the other – the odd sums. Calculations without an initial camber show [35] that the first group of equations produces the lowest value for τ_1.

Since the shape of the considered initial camber corresponds to the form of a "cap" – a single wave of the sinusoid along and across the honeycomb cell plate (Fig. 14), in expression (31), for the initial camber, all terms in the expansion series, except for those corresponding to $m=n=1$, will equal zero. This means that only one term in the series for the initial camber will not equal zero: $f_{0\_11}\neq 0$. To obtain a more accurate approximation for τ_{xy}, one should considered as many equations as possible in the system (31) [35]. By retaining five terms in the series for an elastic camber, we obtain the following system of equations from (31):

$$\begin{cases}
\frac{\pi^4 a_c D}{32h^3\delta\tau_1}\left(1+\frac{h^2}{a_c^2}\right)^2 f_{1_11}-\frac{4}{9}f_{1_22}=0;\\
-\frac{4}{9}f_{1_11}-\frac{4}{9}f_{0_11}+16\frac{\pi^4 a_c D}{32h^3\delta\tau_1}\left(1+\frac{h^2}{a_c^2}\right)^2 f_{1_22}+\\
+\frac{4}{5}f_{1_13}+\frac{4}{5}f_{1_31}-\frac{36}{25}f_{1_33}=0;\\
\frac{4}{5}f_{1_22}+\frac{\pi^4 a_c D}{32h^3\delta\tau_1}\left(1+9\frac{h^2}{a_c^2}\right)f_{1_13}=0;\\
\frac{4}{5}f_{1_22}+\frac{\pi^4 a_c D}{32h^3\delta\tau_1}\left(9+\frac{h^2}{a_c^2}\right)^2 f_{1_31}=0;\\
-\frac{36}{25}f_{1_22}+\frac{\pi^4 a_c D}{32h^3\delta\tau_1}\left(9+\frac{h^2}{a_c^2}\right)^2 f_{1_33}=0.
\end{cases} \quad (32)$$

Let us analyze the effect of the initial technological camber arrow on the general performance of a type I facet, susceptible to shear. The shape of the elastic flexure of the type I facet will be determined by substituting in expression (8) the coefficients, found from the system of equations (32), of expansion into a series of the elastic flexure function for different values of τ_1 at a fixed magnitude of the initial camber arrow.

In contrast to the summing up of the amplitudes of waves of elastic flexure and the initial one under compression stresses, the oblique waves are formed in this case. Their nodes are arranged at an angle so that the plate bends with sharp kinks in the direction of the compressed diagonal (Fig. 15). This almost negates the impact of the initial camber on the performance of a type I facet

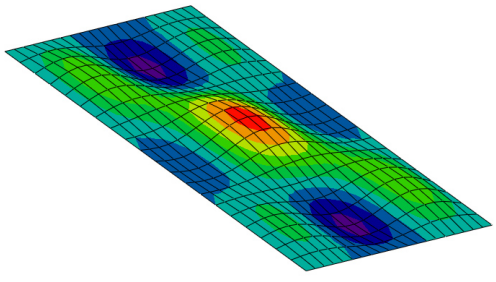

Fig. 15. The shape of elastic bulging of the plate at the arrow of initial camber equal to $f_0=1.4\delta$

To assess the impact of the initial camber arrow on the performance of a type I facet, let us consider the case of its absence, that is $f_0=0$. Given this, the system of equations (32) is transformed into a system of equations obtained by S. P. Timoshenko for a perfect plate in work [34]. Let us build graphs of the dependence of acting stresses τ_1 on elastic flexure w_1 at fixed f_0 and compare them with the critical stresses for the loss of stability by the ideal facet of type I. The expression for critical stresses of stability loss by the ideal type I facet due to shear τ_1 will be derived similarly to the approach given in paper [35], that is by equating the identifier of equation system (32) to zero at $f_0=0$ and by expressing the corresponding τ_{cr1}. Fig. 16 shows, for the central point of the type I facet, the qualitative character of the resulting graphs.

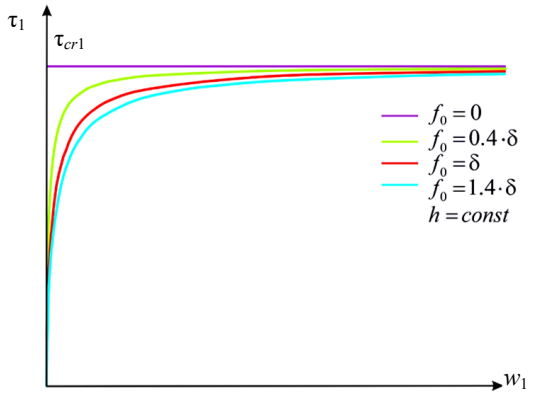

Fig. 16. Qualitative character of the graphs of dependence τ_1 on elastic flexure w_1 at fixed magnitudes f_0 at the central point of a type I facet

It follows from the analysis of Fig. 16 that graphs of dependence of acting stresses τ_1 on elastic flexure w_1 for different magnitudes of arrows of the initial camber f_0 asymptomatically tend to the magnitude of critical ones, τ_{cr1}, for the considered type I facet without the initial camber as

early as at low magnitudes for an elastic flexure. This means that insignificant difference between magnitudes τ_{cr1} and τ_1 will only be observed at the initial stages of loading; the subsequent loading would result in $\tau_1 \approx \tau_{cr1}$. This performance of the type I facet with the initial technological camber is due to its shape in the form of a "cap" (a single wave of the sinusoid surface of the initial camber in the direction of x and y axes): the effect of the shape of the considered technological camber in the system of equations (32) is represented by only one term in the series f_{0_11}.

It follows from the foregoing that in determining the physical-mechanical characteristics of a cellular filler at shear one can neglect the presence in its facets of the considered shape of the initial technological camber.

7. Discussion of results of studying the effect of technological camber of a cellular filler's facets on its physical and mechanical characteristics

Our study into the impact of the initial technological camber in the facets of a cellular filler on its physical and mechanical characteristics has made it possible to develop an approach allowing the prediction of the character of honeycomb structure operation considering the presence of this technological defect. In contrast to available studies [21, 25, 26], a new discrete-element model of the cellular filler was considered, which has made it possible to solve the problem on establishing the mechanism of the effect of the technological camber of honeycomb facets on their physical and mechanical characteristics. A demonstration of the proposed approach has shown a significantly better convergence between the theoretical data obtained with experimental data (Table 1). Thus, for the considered example, the difference between the existing theoretical models [21, 25, 26] and experimental data on the elasticity module under transverse compression was $\left(\Delta_{E_z}\right)_{\min}^{f_0=0} = \frac{E_z^{theor}}{E_{z\max}^{exper}} = \frac{637}{106} \approx 6$ times in the absence of the initial camber of honeycomb cells, and $\left(\Delta_{E_z}\right)_{\min}^{f_0=0.15} = \frac{E_z^{theor} - E_{z\max}^{exper}}{E_{z\max}^{exper}} \approx \frac{430}{106} = 4$ times at f_0=0.15 mm.

Calculation based on the proposed approach has made it possible to obtain discrepancies for the lower boundary of the experiment by 2.61 times, and for the upper one – by 1.1 times. The proposed discrete-element model of a cellular filler and the algorithm that implements have allowed us, for the first time, in contrast to existing models, to explain the significant variation in experimental data. Thus, the resulting diagram "reduced stresses – deformations" of a cellular filler has two sections corresponding to the maximum and minimum carrying capacity of the considered representative element of honeycomb structures. The results from comparing the obtained theoretical range of change in the cellular filler's elasticity module under transverse compression with the lower and upper boundaries of the experiment also demonstrate the validity of the proposed approach.

For the longitudinal shear of a cellular filler, our study has confirmed the assumption, not proven in papers [21, 25, 26], on the absence of impact at shear on honeycomb structure operation from the arrow of the considered technological camber. Accordingly, to determine the shear modules G_{xz}, G_{yz} of honeycomb structures, if they have the initial technological camber in their facets, one can use existing analytical dependences [21, 25, 26].

It appears justified to give some recommendations to the synthesis of the results obtained in determining the physical-mechanical characteristics of a cellular filler within the framework, proposed in papers [8, 12], of the concept on minimizing the mass of composite assemblies in the aviation and rocket and space industry. The concept of mass minimization, proposed in those papers, makes it possible to take into consideration the deterioration in the physical and mechanical characteristics of a cellular filler, caused by the presence of such an inevitable technological deviation in it as the initial technological camber of honeycomb structures. Thus, for one of the verification units of the proposed optimization concept, one can use, as one of the modules, a module to account for the presence of the initial technological camber in the facets of honeycomb structures. The proposed algorithm for implementing such an optimization unit can be represented in the following form:

1. As a regulated tolerance for the technological deviations of a cellular filler, to accept the recommendations from paper [33] on the margins of tolerances for the magnitude of the initial technological camber of honeycomb facets: $0.4\delta \le f_0 \le 1.4\delta$.

2. By using the proposed algorithm, a chart of the deformation of honeycomb structures is constructed $\sigma_{redz} - \varepsilon_z$, reflecting the character of its operation under a phased transverse compression, taking into consideration the presence of the initial technological camber in its facets.

3. The resulting graph is introduced to the software suite of finite-element analysis for the generated model of the optimal variant of the composite sandwich-type structure for a cellular filler. The introduced deformation diagram characterizes the dependence of stresses on deformations in a non-linear statement, because the calculations carried out with it require an iterative process. The limitations for the carrying capacity of a cellular filler with a technological camber to be accepted in such a verification unit is the limit of strength of honeycomb structures under transverse compression, found in accordance with the devised recommendations. In this case, the physical and mechanical characteristics of honeycomb structures do not change at shear.

4. A non-linear analysis is performed for the optimal variant of a composite sandwich-type structure with a cellular filler in accordance with the deformation chart introduced $\sigma_{redz} - \varepsilon_z$.

5. A conclusion is made about the carrying capacity of the optimal variant on terms of mass of the composite sandwich-type structure with a cellular filler, taking into consideration the presence in its facets of the initial technological camber within the regulated tolerance.

Such a synthesis of the results obtained on refining the physical and mechanical characteristics of honeycomb structures and the methods of optimizing their design parameters at the current level of their production technology would make it possible to eventually implement almost exhaustive possibilities of this type of the filler.

8. Conclusions

1. For a gradual loading with transverse compression and shear of a cellular filler, an analysis has been performed of the performance of separate elements of its cell in the presence of the initial technological camber in them. Our analysis of performance by individual elements of a honeycomb cell in

the presence of the initial technological camber in them has made it possible to take into consideration the patterns in the operation of each of them by constructing a filler deformation diagram corresponding to the type of loading. This solved the task on establishing the mechanism of influence of the technological camber of honeycomb facets on their physical and mechanical characteristics.

2. An approach has been developed that has allowed us to predict the character of operation of a cellular filler, taking into consideration the patterns in the perception of load by individual elements of honeycomb cell in the presence of the initial technological camber in them within the regulated tolerance. Based on this, an algorithm has been constructed to determine the physical and mechanical characteristics of a cellular filler under transverse compression, taking into consideration the presence of the initial technological camber in its facets. For the longitudinal shear of a cellular filler, we have carried out analysis of performance of individual elements in a honeycomb cell in the presence of the initial technological camber in them. The results from analysis have confirmed the assumption, which was not proven in a series of papers, that there was no impact at shear on the operation of cellular filler arrow of the considered technological camber. In accordance with this, the conclusion was made about the independence of the physical-mechanical characteristics of a cellular filler at shear on the magnitude of the arrow of the initial technological camber.

References

1. Nunes, J. P., Silva, J. F. (2016). Sandwiched composites in aerospace engineering. Advanced Composite Materials for Aerospace Engineering, 129–174. doi: https://doi.org/10.1016/b978-0-08-100037-3.00005-5
2. Fomin, O., Gerlici, J., Lovskaya, A., Kravchenko, K., Prokopenko, P., Fomina, A., Hauser, V. (2018). Research of the strength of the bearing structure of the flat wagon body from round pipes during transportation on the railway ferry. MATEC Web of Conferences, 235, 00003. doi: https://doi.org/10.1051/matecconf/201823500003
3. Panin, V. F., Gladkov, Yu. A. (1991). Konstruktsii s zapolnitelem. Moscow: Mashinostroenie, 272.
4. Herrmann, A. S.; Virson, J. R. (Ed.) (1999). Design and Manufacture of Monolithic Sandwich Structures with Cellular Cares. Stockholm, 274.
5. Dutton, S., Kelly, D., Baker, A. (2004). Composite Materials for Aircraft Structures. American Institute of Aeronautics and Astronautics Inc., Reston. Virginia, 599. doi: https://doi.org/10.2514/4.861680
6. Slyvynskyi, V. I., Sanin, A. F., Kharchenko, M. E., Kondratyev, A. V. (2014). Thermally and dimensionally stable structures of carbon-carbon laminated composites for space applications. Proceedings of the International Astronautical Congress, IAC 65. Toronto, Canada, 8, 5739–5751.
7. Gaidachuk, V. E., Kondratiev, A. V., Chesnokov, A. V. (2017). Changes in the Thermal and Dimensional Stability of the Structure of a Polymer Composite After Carbonization. Mechanics of Composite Materials, 52 (6), 799–806. doi: https://doi.org/10.1007/s11029-017-9631-6
8. Kondratiev, A., Gaidachuk, V. (2019). Weight-based optimization of sandwich shelled composite structures with a honeycomb filler. Eastern-European Journal of Enterprise Technologies, 1 (1 (97)), 24–33. doi: https://doi.org/10.15587/1729-4061.2019.154928
9. Fomin, O., Gerlici, J., Lovska, A., Kravchenko, K., Prokopenko, P., Fomina, A., Hauser, V. (2019). Durability Determination of the Bearing Structure of an Open Freight Wagon Body Made of Round Pipes during its Transportation on the Railway Ferry. Communications-Scientific letters of the University of Zilina, 21 (1), 28–34.
10. Ivanov, A. A., Kashin, S. M., Semenov, V. I. (2000). Novoe pokolenie sotovyh zapolniteley dlya aviatsionno-kosmicheskoy tehniki. Moscow: Energoatomizdat, 436.
11. Slyvyns'kyy, V., Slyvyns'kyy, M., Polyakov, N. et. al. (2008). Scientific fundamentals of efficient adhesive joint in honeycomb structures for aerospace applications. 59th International Astronautical Congress 2008.
12. Slyvyns'kyy, V., Gajdachuk, V., Kirichenko, V., Kondratiev, A. (2012). Basic parameters' optimization concept for composite nose fairings of launchers. 62nd International Astronautical Congress, 9, 5701–5710.
13. Kondratiev, A., Slivinsky, M. (2018). Method for determining the thickness of a binder layer at its non-uniform mass transfer inside the channel of a honeycomb filler made from polymeric paper. Eastern-European Journal of Enterprise Technologies, 6 (5 (96)), 42–48. doi: https://doi.org/10.15587/1729-4061.2018.150387
14. Sypeck, D. J. (2005). Wrought aluminum truss core sandwich structures. Metallurgical and Materials Transactions B, 36 (1), 125–131. doi: https://doi.org/10.1007/s11663-005-0012-5
15. Slyvynskyi, V. I., Alyamovskyi, A. I., Kondratjev, A. V., Kharchenko, M. E. (2012). Carbon honeycomb plastic as light-weight and durable structural material. 63th International Astronautical Congress, 8, 6519–6529.
16. Gaydachuk, A. V., Slivinsky, M. V., Golovanevsky, V. A. (2006). Technological Defects Classification System for Sandwiched Honeycomb Composite Materials Structures. Materials Forum, 30, 96–102.
17. Barabash, A. V., Gavril'chenko, E. Y., Gribkov, E. P., Markov, O. E. (2014). Straightening of sheet with correction of waviness. Steel in Translation, 44 (12), 916–920. doi: https://doi.org/10.3103/s096709121412002x
18. Kondratiev, A., Gaidachuk, V., Nabokina, T., Kovalenko, V. (2019). Determination of the influence of deflections in the thickness of a composite material on its physical and mechanical properties with a local damage to its wholeness. Eastern-European Journal of Enterprise Technologies, 4 (1 (100)), 6–13. doi: https://doi.org/10.15587/1729-4061.2019.174025

19. Wang, D., Bai, Z. (2015). Mechanical property of paper honeycomb structure under dynamic compression. Materials & Design, 77, 59–64. doi: https://doi.org/10.1016/j.matdes.2015.03.037
20. Gritskiv, L. N. (2005). Ob opredelenii kriticheskih napryazheniy poteri ustoychivosti sotovogo zapolnitelya. Voprosy proektirovaniya i proizvodstva konstruktsiy letatel'nyh apparatov, 3 (42), 76–81.
21. Birger, I. A., Panovko, Ya. G. (Eds.) (1968). Prochnost', ustoychivost', kolebaniya. Vol. 2. Moscow: Mashinostroenie, 463.
22. Gaydachuk, V., Koloskova, G. (2016). Mathematical modeling of strength of honeycomb panel for packing and packaging with regard to deviations in the filler parameters. Eastern-European Journal of Enterprise Technologies, 6 (1 (84)), 37–43. doi: https://doi.org/10.15587/1729-4061.2016.85853
23. Kondratiev, A., Prontsevych, O. (2018). Stabilization of physical-mechanical characteristics of honeycomb filler based on the adjustment of technological techniques for its fabrication. Eastern-European Journal of Enterprise Technologies, 5 (1 (95)), 71–77. doi: https://doi.org/10.15587/1729-4061.2018.143674
24. Slivinsky, M., Slivinsky, V., Gajdachuk, V. et. al. (2004). New Possibilities of Creating Efficient Honeycomb Structures for Rockets and Spacrafts. 55th International Astronautical Congress of the International Astronautical Federation, the International Academy of Astronautics, and the International Institute of Space Law. doi: https://doi.org/10.2514/6.iac-04-i.3.a.10
25. Slyvyns'kyy, V., Gajdachuk, V., Gajdachuk, A., Slyvyns'ka, N. (2005). Weight optimization of honeycomb structures for space applications. 56th International Astronautical Congress of the International Astronautical Federation, the International Academy of Astronautics, and the International Institute of Space Law. doi: https://doi.org/10.2514/6.iac-05-c2.3.07
26. Slyvyns'kyy, V., Gajdachuk, A., Melnikov, S. M. et. al. (2007). Technological possibilities for increasing quality of honeycomb cores used in aerospace engineering. 58th International Astronautical Congress 2007 Hyderabad.
27. Kondrat'ev, A. V., Gritskiv, L. N. (2007). Opredelenie modulya normal'noy uprugosti sotovogo zapolnitelya pri poperechnom szhatii s uchetom nachal'nogo tehnologicheskogo nesovershenstva fol'gi. Voprosy proektirovaniya i proizvodstva konstruktsiy letatel'nyh apparatov, 51 (4), 131–139.
28. Gaydachuk, V. E., Kondrat'ev, A. V., Kirichenko, V. V., Slivinskiy, V. I. (2011). Optimal'noe proektirovanie kompozitnyh sotovyh konstruktsiy aviakosmicheskoy tehniki. Kharkiv: Nats. aehrokosm. un-t «Khark. aviats. in-t», 172.
29. Mackerle, J. (2002). Finite element analyses of sandwich structures: a bibliography (1980–2001). Engineering Computations, 19 (2), 206–245. doi: https://doi.org/10.1108/02644400210419067
30. Fomin, O., Logvinenko, O., Burlutsky, O., Rybin, A. (2018). Scientific Substantiation of Thermal Leveling for Deformations in the Car Structure. International Journal of Engineering & Technology, 7 (4.3), 125–129. doi: https://doi.org/10.14419/ijet.v7i4.3.19721
31. Frulloni, E., Kenny, J. M., Conti, P., Torre, L. (2007). Experimental study and finite element analysis of the elastic instability of composite lattice structures for aeronautic applications. Composite Structures, 78 (4), 519–528. doi: https://doi.org/10.1016/j.compstruct.2005.11.013
32. Slyvyns'kyy V., Slyvyns'kyy M. et. al. (2006). New concept for weight optimization of launcher nose firings made of honeycomb structures. 57th International Astronautical Congress. doi: https://doi.org/10.2514/6.iac-06-c2.p.1.11
33. Kirichenko, V. V., Mel'nikov, S. M. (2006). Faktory, opredelyayushchie tehnologicheskuyu pogib' graney yacheek sotovogo zapolnitelya iz metallicheskoy fol'gi i vozmozhnosti ee normirovaniya. Voprosy proektirovaniya i proizvodstva konstruktsiy letatel'nyh apparatov, 2, 62–70.
34. Timoshenko, S. P. (1971). Ustoychivost' cterzhney, plastin i obolochek. Moscow: Nauka, 807.
35. Donnell, L. H. (1976). Beams Plates and Shells. McGraw-Hill, 453.
36. Beer, F. P. (2009). Mechanics of materials. McGraw-Hill Higher Education, 782.
37. Slivinskiy, V. I. (1996). Eksperimental'noe issledovanie fiziko-mehanicheskih harakteristik sotov. Voprosy proektirovaniya i proizvodstva konstruktsiy letatel'nyh apparatov, 30–43.